Low-energy gamma-ray observations above 1 GeV with CALET on the International Space Station

Nicholas Cannady[a,b,c,*] on behalf of the CALET Collaboration
(a complete list of authors can be found at the end of the proceedings)

[a] *Center for Space Sciences and Technology,*
University of Maryland, Baltimore County,
1000 Hilltop Circle, Baltimore, Maryland 21250, USA

[b] *Astroparticle Physics Laboratory,*
NASA/GSFC,
Greenbelt, Maryland 20771, USA

[c] *Center for Research and Exploration in Space Sciences and Technology,*
NASA/GSFC,
Greenbelt, Maryland 20771, USA

E-mail: ncannady@umbc.edu

The CALorimetric Electron Telescope (CALET) was launched in August 2015 and installed on the International Space Station (ISS) Japanese Experiment Module Exposed Facility. Alongside the primary science targets of GeV—TeV energy cosmic-ray electrons and cosmic-ray hadrons up to PeV energies, CALET is sensitive to gamma rays from 1 GeV up to 10 TeV, limited by statistics. Access to energies below 10 GeV is enabled by a dedicated low-energy gamma (LE-γ) trigger which is active only at low geomagnetic latitudes. In this work we review the analysis of gamma-ray events collected with this trigger including the mitigation of a secondary photon background from cosmic-ray interactions with ISS structures in the CALET field-of-view, the observation of persistent galactic and extragalactic sources, and the detection of emission from the quiescent Sun.

*37*th *International Cosmic Ray Conference (ICRC 2021)*
July 12th – 23rd, 2021
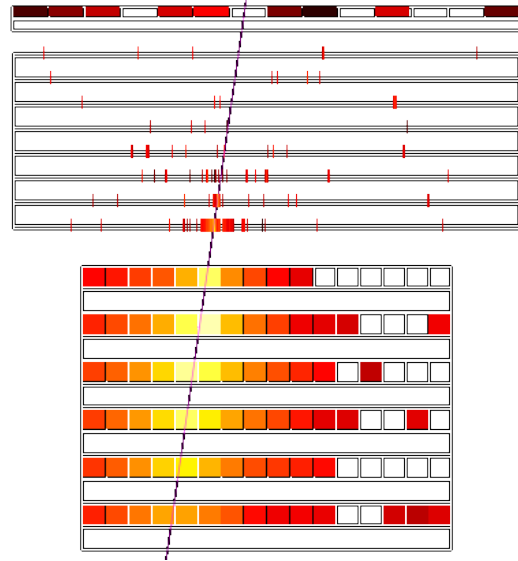*Online – Berlin, Germany*

---

[*]Presenter

1. Gamma-ray analysis with the CALET calorimeter

The Calorimetric Electron Telescope (CALET) was launched in August 2015 from Tanegashima Space Center in Japan to the Japanese Experiment Module Exposed Facility (JEM-EF) on the International Space Station (ISS). Scientific operations have continued stably from October 2015 to date and are approved until at least the end of 2024. CALET was primarily designed to measure the cosmic-ray electron spectrum from 10 GeV well into the TeV energies. Given the similarity between electron- and photon-induced electromagnetic showers, CALET is also sensitive to gamma rays in this energy range.

The primary instrument on CALET is the 30 radiation length (X_0) deep electromagnetic calorimeter (CAL) [1] (see Figure 1). The CAL comprises three subsystems: a charge detector (CHD) made of one x- and one y-layer of plastic scintillating paddles; an imaging calorimeter (IMC) made of eight pairs of x- and y-layers of plastic scintillating fibers separated by seven tungsten sheets (total $3X_0$) which stimulate shower development; and a total absorption calorimeter (TASC) made of 12 layers of lead tungstate logs (total $27X_0$) which can fully absorb electromagnetic showers at TeV energies. The


Figure 1: A sample gamma-ray event in the calorimeter. The reconstructed track based on the energy deposits in the IMC and the clean charge zero measurement in the CHD are shown. The primary energy is reconstructed based on the IMC and TASC energy deposits based on simulations of events in the same geometrical acceptance condition.

calorimeter is only 1.3 proton interaction lengths deep, and the large difference in electron radiation length depth and proton interaction length depth creates a difference in shower topologies for electron or photon primaries as compared to those from hadronic primaries.

In additional to the high-energy (HE) trigger observations in the energy range above, CALET also measures photons down to 1 GeV with a dedicated low-energy gamma (LE-γ) trigger [2]. The LE-γ trigger is active specifically at low geomagnetic latitudes, where low-energy charged particles are deflected by the geomagnetic field and background rates are therefore kept at a manageable level. A selection algorithm for events seen with this trigger has been implemented and the instrument response has been characterized and validated [3]. For these low-energy events, the pathlength in the TASC needed for absorption of the shower energy is shorter, and the geometrical acceptance conditions for the LE-γ analysis allow much wider angles of incidence (field-of-view (FOV) reaching ~60°). This increase in geometrical factor is countered, however, by the requirement that the trajectory pass through the CHD for clear charge 0 selection, leading to a geometrical factor of ~1000 cm²sr, comparable with the total standard acceptance. For energy spectra shown in this work, the absolute energy scale correction of 3.5% as derived by analyzing changes in the low-energy electron spectrum as a function of geomagnetic rigidity cutoff [4] is applied.

Although here we focus on the low-energy observations (for analysis focused on the HE trigger,

see [5]), we include data taken with the HE trigger as well to extend results above 10 GeV. Note that these data are taken with a limited geometrical acceptance (similar to that used for the electron analysis), and that selections are being studied in detail for the possible improvement of the HE trigger geometrical factor for photons. Furthermore, we do not discuss here the important topic of fast transient event follow-up (e.g. GRBs and gravitational wave events); for discussion of those analyses see [6]. An overview of other CALET results can be seen in the highlight report [1].

2. Data analysis

For this work, the complete CALET Pass 4.1 dataset is used, representing the most up-to-date calibrations (including those in [7] and others) and covering the time period from 2015/11/01 (when the LE-γ trigger was first activated) to 2020/09/30 for a total of 1796 days. Data are converted from their Level 1 format to Level 2 (event reconstruction and calibrations are applied) at the Waseda CALET Operations Center (WCOC) at Waseda University in Tokyo, Japan.

An important source of background events for the gamma-ray analysis in CALET is due to transient and permanent structures from other ISS and JEM-EF systems impinging on the CAL FOV, especially at the periphery. An example month (2016/08) with a variety of obstructions is shown in Figure 2. Cosmic rays interact with these structures and produce a bright secondary photon signal that must be removed in order to clean the dataset. Permanent structures (e.g.
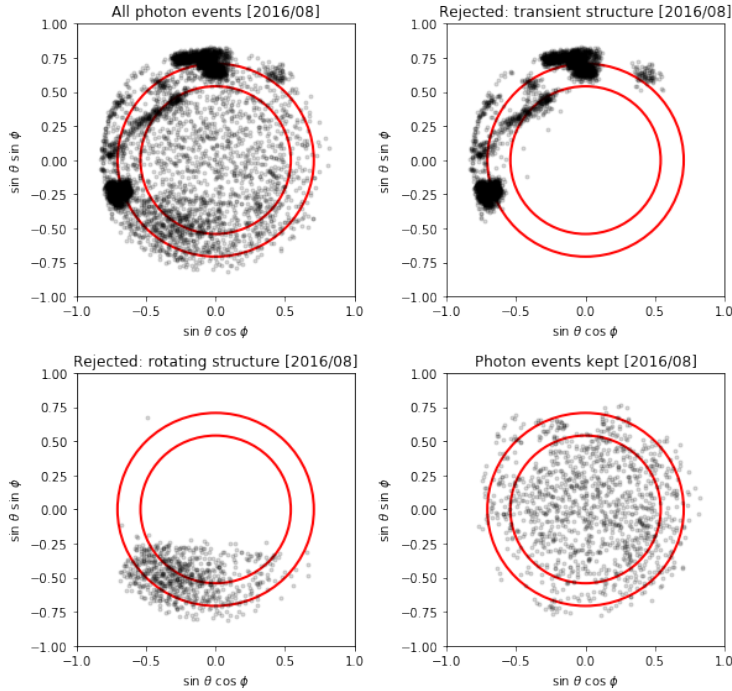
Figure 2: Effects of the FOV cuts for the month of August 2016. Robotic arm activity impinged on the upper left region for four days. *upper left:* all LE photon candidates, *upper right:* events rejected by the manually-defined structure cuts, *bottom left:* events rejected by the ray-tracing model code, and *bottom right:* events kept for analysis. Red circles denote 45° and 60° from zenith.

payload mounting fixture) and structures that rotate predictably (e.g. solar panels or radiators) are modeled with ray tracing code provided by JAXA. Transient structures (e.g. the SSRMS or JEM-RMS robotic arms) are removed through communication with ISS operations notes and manual inspection of photon event distributions in the FOV in time periods when obstructions are known to be present. Maps of rejected FOV regions for each time period are defined, synchronized to the central WCOC calibration database, and used in the processing of high-level analysis files. While these obstructions have little effect on high-energy cosmic rays and are typically outside of the geometrical acceptance for cosmic-ray analysis (extending to ~45°; the red circles in Figure 2 indicate 45° and 60° from zenith, for reference), the generation of GeV-energy secondary photons and the more open acceptance conditions for the LE-γ trigger makes their removal essential for
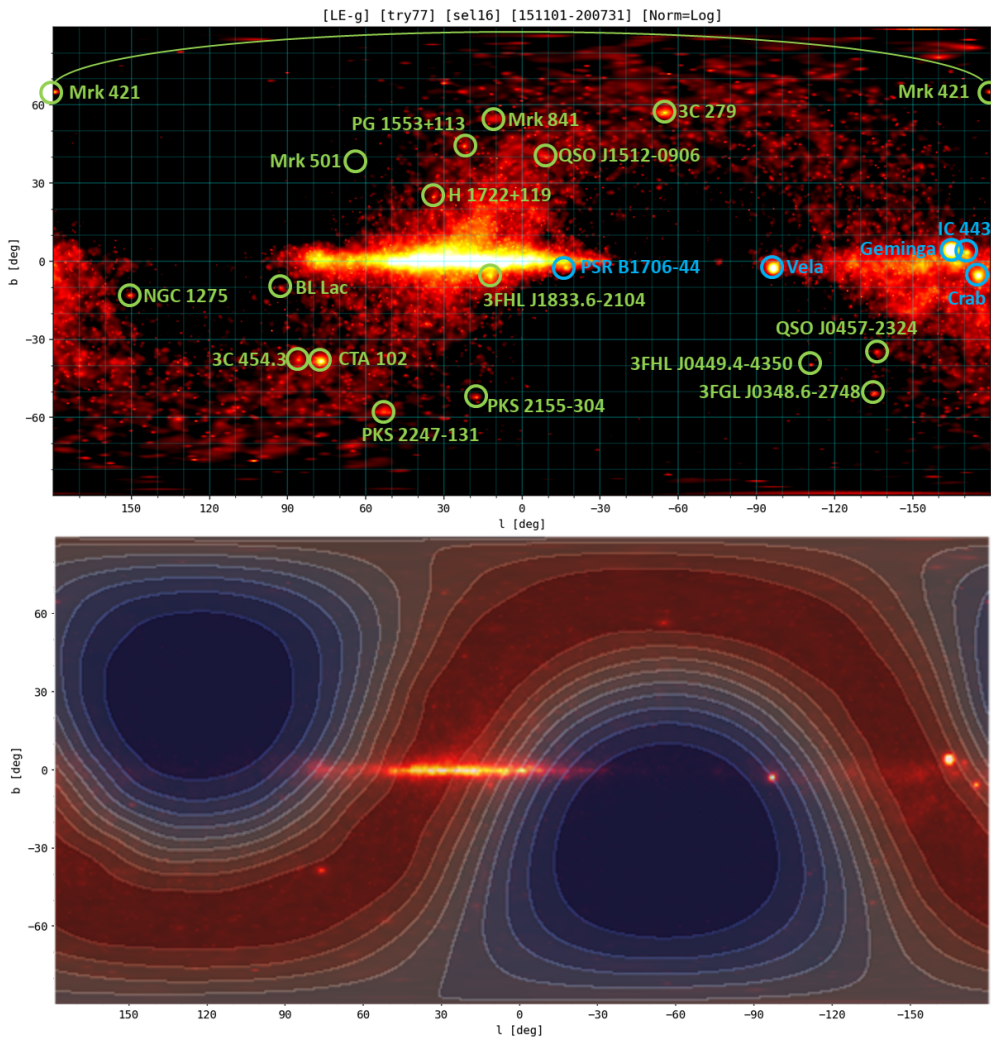
Figure 3: LE-γ trigger skymaps. *top*: counts map smeared by the instrument response functions shown in a logarithmic scale. Sources with excess events at their known locations are indicated by circles and labels (blue: galactic, green:extragalactic). *bottom*: counts map overlaid with exposure contours incremented by 10% relative to the maximum exposure.

analysis of gamma rays in the CAL.

The high-level analysis files are reduced from Level 2 to include photon-specific selection information, reconstructed energies, and exposures, accounting for the effects of the previously discussed ISS structures. The results reported below are derived based on this reduced dataset.

3. Observation overview

Figure 3 summarizes the LE-γ observations over five years of observations. The point-spread function (PSF) is determined for each photon event and an order 9 Healpix map is filled with the summed smeared signals from each. The total exposure is accumulated in bins of energy for each pixel of an order 6 Healpix map. The top panel in Figure 3 shows the resulting counts map in logarithmic scaling. Sources detected in the CALET dataset are marked by green or blue circles depending on extragalactic or galactic origin, respectively. The significance level of the detection of each source is still under evaluation. The bottom panel shows the exposure on the sky for the LE-γ trigger relative to the maximum value at 5 GeV ($\sim$1.68 $\times 10^9$ cm^{2}s).

## 4. Observations of persistent point sources
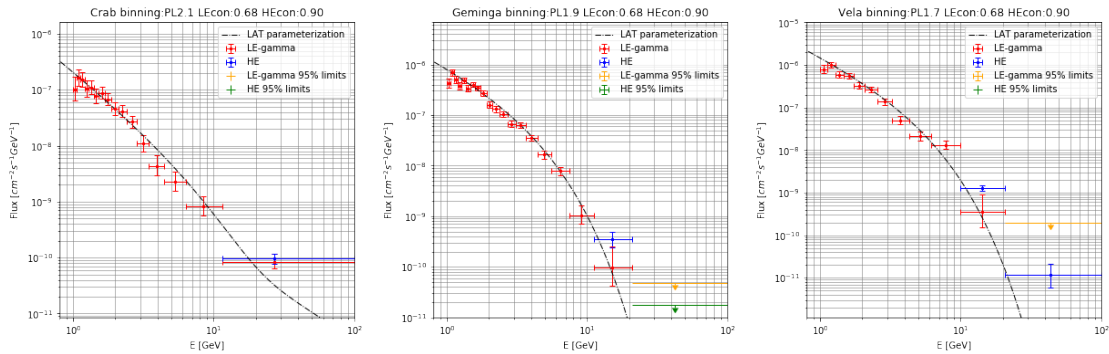
Figure 4: Spectra for bright galactic sources (*from left*: Crab, Geminga, and Vela. Black dotted lines show fitted results from *Fermi* LAT ([8], [9], [10]).

Measurement of the fluxes from bright point sources and the stability of these results are an important validation of gamma-ray analysis in the CAL. The brightest of these sources are the Crab, Geminga, and Vela, whose energy spectra are shown in Fig. 4. The binning was chosen to balance the energy resolution in the CAL with the statistics afforded by the exposure and spectral shape of each source. The results extend those in [3] to beyond 10 GeV. Results from the HE trigger are included, shown in the figures with the blue data points. Model results from *Fermi* LAT are shown for comparison, and are in good agreement with the presented results.

Some sources in the CALET dataset have been seen to exhibit flaring activity, most notable from the active galactic nucleus (AGN) CTA 102. The counts map and light curve for CTA 102 as seen by CALET are shown in Figure 5. The right panel shows that the majority of the signal from CTA 102 was concentrated in the six month period 2016/11 - 2017/05. After the end of the

flaring period, no further high-energy (E > 10 GeV) was seen in from the source, and in fact, the majority of events detected from the source since 2017/05 are very low energy (E < 2 GeV). The left panel shows the source well-separated from the background over the full five years of observation, emphasizing the strength of the flare given the diminished subsequent flux.
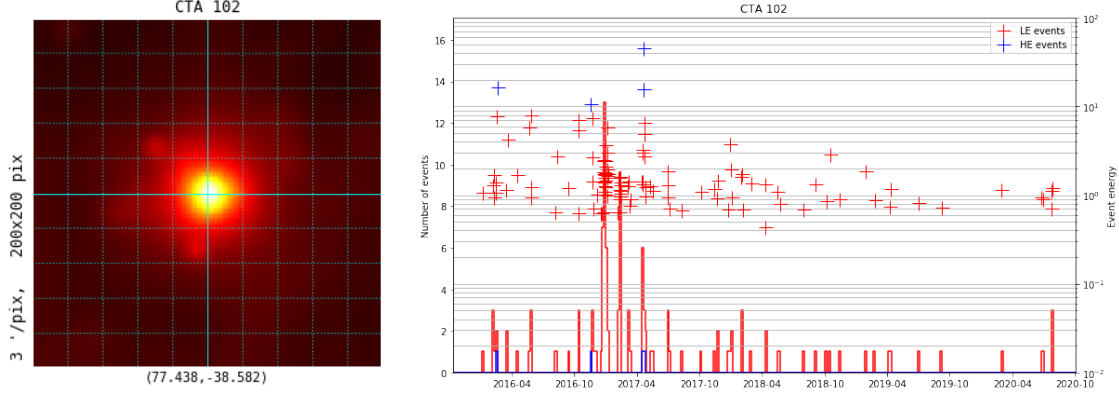
Figure 5: Observations of CTA 102. *left:* count map centered at the CTA 102 position. *right:* light curve with 10 day bins of CTA 102 over the full observation period (counts on left y-axis). Individual events are marked with crosses as a function of time and energy (right y-axis).

Other sources detected in the five-year dataset can be attributed primarily to flares as well. ~20% of all photons detected by CALET from the AGN 3C 279 were seen within a two week period in early 2018. On the other hand, emission from 3FHL J1833.6-2104 was infrequent until late 2018, and then increased by a factor of ~3 thereafter. The changes in energy spectra for these flaring sources based on the CALET data are still under evaluation.

5. Detection of GeV-energy emission from the quiescent Sun

Non-thermal emission from the Sun in quiescence was predicted based on cosmic-ray inter-actions near the photosphere [11]. In addition, an extended halo is also predicted due to inverse Compton scattering of the photon field by cosmic-ray electrons [12]. These two components were detected in EGRET data [13] and later by *Fermi* LAT [14]. Later analyses using *Fermi* LAT data over a longer period revealed an unexpected, significant dip in the disk spectrum between 30-50 GeV [15] and the potential presence of a mechanism driving emission up to hundreds of GeV [16] correlated with the Solar cycle. With this in mind, we aim to study this Solar emission using CALET observations.

For each candidate event, we rotate its arrival direction based on the position of the Sun at the time of detection. Using the Sun direction as the new z-axis and the ecliptic North pole as the new x-axis, the rotation is defined. Exposures are accumulated daily, and the exposure map is rotated according to the Sun's position at noon UTC on each day. Note that this rotation does not maintain a constant direction for the Sun's rotational axis, but a morphological study is already infeasible at this stage of analysis due to statistical limitations.

The results of a simple event selection around the Solar disk are shown in Figure 6 (error bars are statistical only). This preliminary result shows a featureless power law with index 2. No
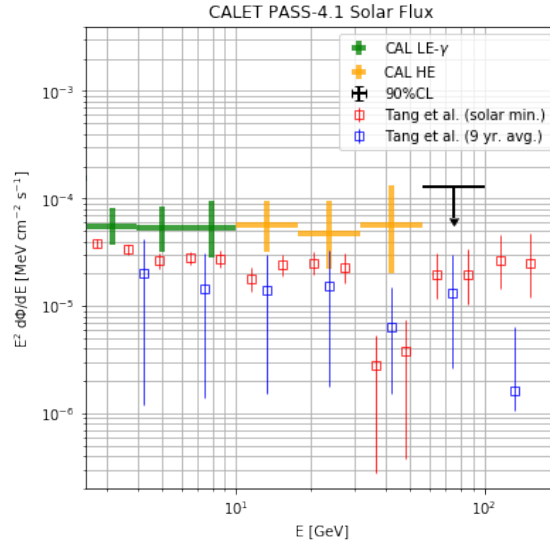
Figure 6: Preliminary measurement of the Solar disk emission using a simple event selection and total of daily exposures. Error bars are statistical only.

evidence is found for the presence of the spectral dip at 30-50 GeV, but given the size of the errors, it is also not significantly precluded. Note as well that this treatment will contain contamination from the inverse Compton component, and a joint fitting of three components (diffuse background, disk, and inverse Compton halo) is in development alongside a dedicated increase of the geometrical factor for the HE gamma-ray analysis.

6. Summary

CALET is making gamma-ray observations from energies E ~ 1 GeV, and has accumulated over five years of data to date with continuous, stable operations. Observational results of point sources are consistent with expectations based on results from *Fermi* LAT, building confidence in the analysis of gamma-ray sources and the treatment of backgrounds, including the significant contamination of the dataset from cosmic-ray induced secondary photons from ISS structures in the CALET FOV.

We presented here the status of several ongoing analysis efforts, including the detection and analysis of persistent sources, the monitoring of transient outbursts from known systems, and the analysis of GeV-energy gamma-ray emission from the quiescent Sun. These results complement those based primarily in detection of counterpart GeV emission from GRBs and gravitational wave sources [6] and in analysis of the HE trigger events for dark matter line searches [5] among others. These efforts are being continued, along with an investigation aiming to expand the HE trigger acceptance for gamma-ray events to extend the results on the Solar gamma-ray analysis. CALET is approved for operations at least through the end of 2024, by which time a dataset exceeding nine years will be achieved.

Acknowledgements

References

[1] P. S. Marrocchesi et al. (CALET Collaboration) in *Proceedings of Science (ICRC2021; this conference)* 786, (2021).

[2] Y. Asaoka, S. Ozawa, and S. Torii et al. (CALET Collaboration), *Astropart. Phys.* 100, 29-37 (2018).

[3] N. Cannady, Y. Asaoka et al. (CALET Collaboration), *Astrophys. J. Supp. Ser.* 238:5, 16pp (2018).

[4] O. Adriani et al. (CALET Collaboration), *Phys. Rev. Lett.* 119, 181101 (2017).

[5] M. Mori et al. (CALET Collaboration) in *Proceedings of Science (ICRC2021; this conference)* 517, (2021).

[6] Y. Kawakubo et al. (CALET Collaboration) in *Proceedings of Science (ICRC2021; this conference)* 817, (2021).

[7] Y. Asaoka, Y. Akaike, Y. Komiya, R. Miyata, S. Torii et al. (CALET Collaboration), *Astropart. Phys.* 91, 1-10 (2017).

[8] A. A. Abdo et al. (Fermi LAT Collaboration), *Astrophys. J.* 708, 1254-1267 (2010).

[9] A. A. Abdo et al. (Fermi LAT Collaboration), *Astrophys. J.* 720, 272-283 (2010).

[10] A. A. Abdo et al. (Fermi LAT Collaboration), *Astrophys. J.* 696, 1084-1093 (2009).

[11] D. Seckel, T. Stanev, T. K. Gaisser, *Astrophys. J.* 382, 652-666 (1991).

[12] I. V. Moskalenko, T. A. Porter, S. W. Digel, *Astrophys. J.* 652, L65-L68 (2006).

[13] E. Orlando and A. W. Strong, *Astron. Astrophys.* 480, 847-857 (2008).

[14] A. A. Abdo et al. (Fermi LAT Collaboration), *Astrophys. J.* 734, 116-125 (2011).

[15] Q.-W. Tang, et al., *Phys. Rev. D* 98, 063019 (2018).

[16] T. Linden et al., *Phys. Rev. Lett.* 121, 131103 (2018).

Full Authors List: CALET Collaboration

O. Adriani[1,2], Y. Akaike[3,4], K. Asano[5], Y. Asaoka[5], E. Berti[1,2], G. Bigongiari[6,7], W. R. Binns[8], M. Bongi[1,2], P. Brogi[6,7], A. Bruno[9,10], J. H. Buckley[8], N. Cannady[11,12,13], G. Castellini[14], C. Checchia[6], M. L. Cherry[15], G. Collazuol[16,17], K. Ebisawa[18], A. W. Ficklin[15], H. Fuke[18], S. Gonzi[1,2], T. G. Guzik[15], T. Hams[11], K. Hibino[19], M. Ichimura[20], K. Ioka[21], W. Ishizaki[5], M. H. Israel[8], K. Kasahara[22], J. Kataoka[23], R. Kataoka[24], Y. Katayose[25], C. Kato[26], N. Kawanaka[27,28], Y. Kawakubo[15], K. Kobayashi[3,4], K. Kohri[29], H. S. Krawczynski[8], J. F. Krizmanic[11,12,13], J. Link[11,12,13], P. Maestro[6,7], P. S. Marrocchesi[6,7], A. M. Messineo[30,7], J.W. Mitchell[12], S. Miyake[32], A. A. Moiseev[33,12,13], M. Mori[34], N. Mori[2], H. M. Motz[35], K. Munakata[26], S. Nakahira[18], J. Nishimura[18], G. A. de Nolfo[9], S. Okuno[19], J. F. Ormes[36], N. Ospina[16,17], S. Ozawa[37], L. Pacini[1,14,2], P. Papini[2], B. F. Rauch[8], S. B. Ricciarini[14,2], K. Sakai[11,12,13], T. Sakamoto[38], M. Sasaki[33,12,13], Y. Shimizu[19], A. Shiomi[39], P. Spillantini[1], F. Stolzi[6,7], S. Sugita[38], A. Sulaj[6,7], M. Takita[5], T. Tamura[19], T. Terasawa[40], S. Torii[3], Y. Tsunesada[41], Y. Uchihori[42], E. Vannuccini[2], J. P. Wefel[15], K. Yamaoka[43], S. Yanagita[44], A. Yoshida[38], K. Yoshida[22], and W. V. Zober[8]

[1]Department of Physics, University of Florence, Via Sansone, 1, 50019 Sesto, Fiorentino, Italy, [2]INFN Sezione di Florence, Via Sansone, 1, 50019 Sesto, Fiorentino, Italy, [3]Waseda Research Institute for Science and Engineering, Waseda University, 17 Kikuicho, Shinjuku, Tokyo 162-0044, Japan, [4]JEM Utilization Center, Human Spaceflight Technology Directorate, Japan Aerospace Exploration Agency, 2-1-1 Sengen, Tsukuba, Ibaraki 305-8505, Japan, [5]Institute for Cosmic Ray Research, The University of Tokyo, 5-1-5 Kashiwa-no-Ha, Kashiwa, Chiba 277-8582, Japan, [6]Department of Physical Sciences, Earth and Environment, University of Siena, via Roma 56, 53100 Siena, Italy, [7]INFN Sezione di Pisa, Polo Fibonacci, Largo B. Pontecorvo, 3, 56127 Pisa, Italy, [8]Department of Physics and McDonnell Center for the Space Sciences, Washington University, One Brookings Drive, St. Louis, Missouri 63130-4899, USA, [9]Heliospheric Physics Laboratory, NASA/GSFC, Greenbelt, Maryland 20771, USA, [10]Department of Physics, Catholic University of America, Washington, DC 20064, USA, [11]Center for Space Sciences and Technology, University of Maryland, Baltimore County, 1000 Hilltop Circle, Baltimore, Maryland 21250, USA, [12]Astroparticle Physics Laboratory, NASA/GSFC, Greenbelt, Maryland 20771, USA, [13]Center for Research and Exploration in Space Sciences and Technology, NASA/GSFC, Greenbelt, Maryland 20771, USA, [14]Institute of Applied Physics (IFAC), National Research Council (CNR), Via Madonna del Piano, 10, 50019 Sesto, Fiorentino, Italy, [15]Department of Physics and Astronomy, Louisiana State University, 202 Nicholson Hall, Baton Rouge, Louisiana 70803, USA, [16]Department of Physics and Astronomy, University of Padova, Via Marzolo, 8, 35131 Padova, Italy, [17]INFN Sezione di Padova, Via Marzolo, 8, 35131 Padova, Italy, [18]Institute of Space and Astronautical Science, Japan Aerospace Exploration Agency, 3-1-1 Yoshinodai, Chuo, Sagamihara, Kanagawa 252-5210, Japan, [19]Kanagawa University, 3-27-1 Rokkakubashi, Kanagawa, Yokohama, Kanagawa 221-8686, Japan, [20]Faculty of Science and Technology, Graduate School of Science and Technology,, Hirosaki University, 3, Bunkyo, Hirosaki, Aomori 036-8561, Japan, [21]Yukawa Institute for Theoretical Physics, Kyoto University, Kitashirakawa Oiwakecho, Sakyo, Kyoto 606-8502, Japan, [22]Department of Electronic Information Systems, Shibaura Institute of Technology, 307 Fukasaku, Minuma, Saitama 337-8570, Japan, [23]School of Advanced Science and Engineering, Waseda University, 3-4-1 Okubo, Shinjuku, Tokyo 169-8555, Japan, [24]National Institute of Polar Research, 10-3, Midori-cho, Tachikawa, Tokyo 190-8518, Japan, [25]Faculty of Engineering, Division of Intelligent Systems Engineering, Yokohama National University, 79-5 Tokiwadai, Hodogaya, Yokohama 240-8501, Japan, [26]Faculty of Science, Shinshu University, 3-1-1 Asahi, Matsumoto, Nagano 390-8621, Japan, [27]Hakubi Center, Kyoto University, Yoshida Honmachi, Sakyo-ku, Kyoto 606-8501, Japan, [28]Department of Astronomy, Graduate School of Science, Kyoto University, Kitashirakawa Oiwake-cho, Sakyo-ku, Kyoto 606-8502, Japan, [29]Institute of Particle and Nuclear Studies, High Energy Accelerator Research Organization, 1-1 Oho, Tsukuba, Ibaraki 305-0801, Japan, [30]University of Pisa, Polo Fibonacci, Largo B. Pontecorvo, 3, 56127 Pisa, Italy, [31]Astroparticle Physics Laboratory, NASA/GSFC, Greenbelt, Maryland 20771, USA, [32]Department of Electrical and Electronic Systems Engineering, National Institute of Technology, Ibaraki College, 866 Nakane, Hitachinaka, Ibaraki 312-8508, Japan [33]Department of Astronomy, University of Maryland, College Park, Maryland 20742, USA, [34]Department of Physical Sciences, College of Science and Engineering, Ritsumeikan University, Shiga 525-8577, Japan, [35]Faculty of Science and Engineering, Global Center for Science and Engineering, Waseda University, 3-4-1 Okubo, Shinjuku, Tokyo 169-8555, Japan, [36]Department of Physics and Astronomy, University of Denver, Physics Building, Room 211, 2112 East Wesley Avenue, Denver, Colorado 80208-6900, USA, [37]Quantum ICT Advanced Development Center, National Institute of Information and Communications Technology, 4-2-1 Nukui-Kitamachi, Koganei, Tokyo 184-8795, Japan, [38]College of Science and Engineering, Department of Physics and Mathematics, Aoyama Gakuin University, 5-10-1 Fuchinobe, Chuo, Sagamihara, Kanagawa 252-5258, Japan, [39]College of Industrial Technology, Nihon University, 1-2-1 Izumi, Narashino, Chiba 275-8575, Japan [40]RIKEN, 2-1 Hirosawa, Wako, Saitama 351-0198, Japan, [41]Division of Mathematics and Physics, Graduate School of Science, Osaka City University, 3-3-138 Sugimoto, Sumiyoshi, Osaka 558-8585, Japan, [42]National Institutes for Quantum and Radiation Science and Technology, 4-9-1 Anagawa, Inage, Chiba 263-8555, Japan, [43]Nagoya University, Furo, Chikusa, Nagoya 464-8601, Japan, [44]College of Science, Ibaraki University, 2-1-1 Bunkyo, Mito, Ibaraki 310-8512, Japan